RSC Advances

PAPER

Cite this: *RSC Adv.*, 2020, **10**, 21636

Fabrication of superwetting, antimicrobial and conductive fibrous membranes for removing/collecting oil contaminants

Ming Zhang,[a] Chengyu Wang,[b] Yinghua Ma,[a] Xiling Du,[a] Yanhua Shi,[a] Jian Li*[b] and Junyou Shi*[a]

Received 24th March 2020
Accepted 21st May 2020

DOI: 10.1039/d0ra02704a

rsc.li/rsc-advances

In order to remove/collect organic contaminants from polluted water, polypyrrole/silver nanoparticles (PPy/Ag NPs) have been loaded onto spandex fabric using the method of *in situ* redox-oxidation polymerization to achieve a specific membrane. Observations showed that the original hydrophobic fabric became superhydrophilic and superoleophobic underwater (with an underwater oil contact angle (OCA) of 160°). The as-prepared specimen could effectively remove the oil from an oil-in-water emulsion. After further hydrophobic modification, the specimen was transformed into a fabric that possessed durable superhydrophobicity and superlipophilicity (with a water contact angle (WCA) of 159°), which could collect the oil from a water-in-oil emulsion. Apparently, the two types of fibrous membranes completely satisfied the conditions for removing/collecting organic contaminants from opposite types of water/oil mixtures. The durable evaluation results exhibited the outstanding resistance of both fibrous membranes to friction and acidic and basic scouring agents. Additionally, the multifunctional fabric membrane also possessed excellent electrical conductivity and antibacterial activities towards *S. aureus*, *B. subtilis*, and *E. coli*, which will greatly promote developments in the textile industry and provide a bright future for fabric-based materials.

Introduction

Combining textile technology with electronic technology and nanotechnology endows textile products with more auxiliary functions. For instance, nanofibrous fabrics with a good conductivity could be further assembled to act as a flexible electrode, wearable sensor (perceiving the minor variations of strain, pressure, chemical, optical, humidity, *etc.*), antennas, flexible supercapacitors, and energy storage and convertor devices, significantly accelerating the development of smart textiles. Polypyrrole (PPy) with a conjugated double bond is recognized for its conducting, electrochemical and responsive properties. In addition, PPy has many other advantages including a good film-forming ability, strong oxidation resistance and simple synthesis processes,[1–3] offering applications in various fields. Jiang *et al.* reported a PPy-coated fabric membrane serving as the electrode for the sensing electron myogram, which could be applied for use in prosthetic limbs control.[4] Xu *et al.* assembled PPy onto a graphene-coated fabric using the vapor deposition method to prepare a flexible supercapacitor.[5] Furthermore, the remarkable biocompatibility and environmental stability of PPy accelerates its combination with Ag on fabric fibers, which could effectively inhibit the growth of bacteria. Owing to the electroporation effect, the bactericidal activity of substrates coated with conductive PPy/Ag nanoparticles (NPs) could also be significantly improved by applying an appropriate voltage.[6]

The physics related to superwetting (mainly including superhydrophilic, superhydrophobic, superoleophilic, superoleophobic) surfaces have been investigated with a view towards their potential application in a variety of industrial and scientific fields.[7–11] It is not hard to assemble PPy/Ag NPs onto a fabric substrate to achieve an interface with an appropriate hierarchical structure, which is the key to forming superwetting materials. Owing to the advantages of a woven fiber structure, as well as the excellent air/liquid permeability, flexible, stretchable, washable and breathable fabrics have become the better choice for use as a substrate for applications in separation and protection.[12] However, the as-received fabric had no ability to selectively permeate water over oil or *vice versa*, its surface needed further modification to control its wettability.[13] Therefore, the design of nanostructured materials with a high selectively and separation efficiency is crucial to reclaiming the oil/water mixtures from spilled oils and chemical leakages, especially versatile fabric membranes with superwetting properties,

[a]Jilin Provincial Key Laboratory of Wooden Materials Science and Engineering, Beihua University, Jilin 132013, China. E-mail: mattzhming@163.com; junyoushi468@163.com

[b]Key Laboratory of Bio-based Material Science and Technology, Ministry of Education, Northeast Forestry University, Harbin 150040, China. E-mail: wangcy@nefu.edu.cn; donglinlijian@163.com

high selectivities, good repeatability and durability.[14–16] Significantly, the strategy to appropriately build hierarchical structures on fabric surfaces should be determined to satisfy various demands including electric conduction, bacterial inhibition and oil/water separation.

Existing technologies for integrating fabrics with PPy and Ag NPs are *in situ* polymerization, the template method, vapor deposition, the electrochemical process[17–20] and so forth. In this study, PPy/Ag NPs were loaded onto the spandex fabric and these constituted an appropriate hierarchical structure on the fiber surface by *in situ* redox-oxidation polymerization. Interestingly, after treatment the original hydrophobic fabric became superhydrophilic and superoleophobic underwater, and became superhydrophobic and superoleophilic after further hydrophobic modification with octadecyl trichlorosilane (OTS), completely satisfying the opposite types of water/oil separation (*e.g.* water-in-oil emulsion and oil-in-water emulsion). The evaluation results revealed that both fabrics exhibited an outstanding conductivity and antibacterial activity. In the meantime, the PPy/Ag-fabric could serve as a filtration medium to separate the oil-in-water emulsion effectively, while the water-in-oil emulsion could be efficiently separated by the PPy/Ag/OTS-fabric. Apparently, a feasible and simple strategy has been put forward to endow the fabric with multiple functions, such as conductive, superwetting, and antibacterial properties, which will largely expand the development of the textile industry and offer fabric-based materials a promising future.

Experimental

Spandex fabrics (100% polyurethane, PU) were obtained locally. Ethanol, *n*-hexane, chloroform, 1,2-dichloroethane, Span 80 and Tween 80 were purchased from Tianjin Damao Chemical Reagent Factory. $AgNO_3$ (99.8%) and $FeCl_3 \cdot 6H_2O$ (99.5%) were obtained from Tianjin Fuyu Fine Chemical Co., Ltd. Octadecyl trichlorosilane (OTS, 95%) and pyrrole (Py, 99%) were purchased from Shanghai Macklin Biochemical Co., Ltd and Aladdin Reagent (Shanghai) Co., Ltd, respectively. All of the reagents in the experiment were used as received without further purification, and the emulsion mixtures used to evaluate the water/oil separation effect of the product were prepared as follows, 0.32 g Tween 80, 2 mL chloroform and 120 mL water were mixed and stirred for 3 h to acquire a chloroform-in-water emulsion. Next, 0.5 g Span 80, 1 mL water and 114 mL chloroform were mixed and stirred for 3 h to acquire a water-in-chloroform emulsion. Then, 4 mL methylbenzene and 120 mL water were mixed and stirred for 3 h to give a methylbenzene-in-water emulsion, and finally, 0.04 g Span 80, 1 mL water and 100 mL *n*-hexane were mixed and stirred for 3 h to give a water-in-*n*-hexane emulsion.

As described in Fig. 1, fabric specimens (30×30 mm^2) were washed in 2% ethanol aqueous solution in advance, and immersed in 0.4 M pyrrole aqueous solution at ambient temperature under gentle magnetic stirring for 2 h. Then, an equal volume of 0.15 M $FeCl_3$ aqueous solution was added to the above described solution at a temperature of 5 °C and this

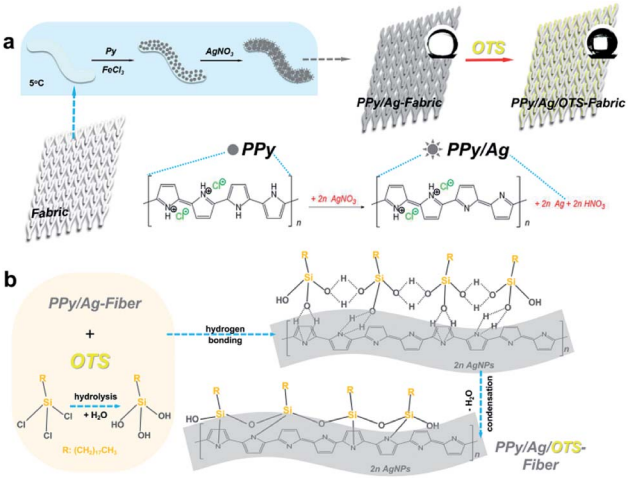

Fig. 1 (a) A schematic illustration of the loading of PPy/Ag NPs onto the fabric specimen; and (b) a reaction mechanism diagram for OTS grafting on the PPy/Ag-fabric specimen.

was allowed to stand for 80 min. After immersion in 2% ethanol aqueous solution and drying at ambient temperature, the polypyrrole (PPy) coated fabrics were acquired. Then, the PPy-coated fabrics were immersed in 0.5 M $AgNO_3$ aqueous solution for 24 h, and dried at ambient temperature to obtaining the PPy/Ag-fabrics with superhydrophilicity and underwater superoleophobicity. Additionally, the selected specimens were immersed in the OTS solution (1%, v/v in *n*-hexane) for 90 min and then rinsed with *n*-hexane. Finally, the PPy/Ag/OTS-fabric with superhydrophobic and superoleophilic properties were obtained after further drying in a vacuum oven at a temperature of 60 °C.

An antimicrobial evaluation of the specimens against *Escherichia coli* (*E. coli*, Gram-negative bacterium), *Staphylococcus aureus* (*S. aureus*, Gram-positive bacterium) and *Bacillus subtilis* (*B. subtilis*, Gram-positive bacterium) has been conducted using the bacterial inhibition ring method. Specifically, the beef extract and peptone in distilled water at pH 7.2 and the empty Petri plates were autoclaved. Then, the beef extract peptone medium was cast into the Petri plates and cooled. The bacterium solution with a dilution degree of 10^{-4} was inoculated on the plates, and then each of the fabric specimens were planted onto the peptone plates. All of the plates were incubated at 28 °C for 16 h. The surface morphology of the specimens was characterized using scanning electron microscopy (SEM, Quanta200), which was operated at 15.0 kV. The compositions of the coatings on the surfaces of the specimens were analyzed using Fourier transform infrared spectroscopy (FTIR, Magna-IR 560). Measurement of the water contact angle (WCA) on the surfaces of the specimens was carried out by utilizing a commercial contact meter (Powreach, JC2000C) at ambient temperature, and the WCA was determined by averaging measurements taken from at least five positions on each specimen.

Results and discussion

At low magnification, the original spandex fabric showed a well-organized knitted structure with numerous micron-sized fibers (Fig. 2a). Fig. 2b shows a randomly selected original fiber from the spandex fabric at high magnification, showing its smooth and flat surface without any bumps or pits. After loading the PPy/Ag NPs, the fiber structure became rougher than the original as shown in Fig. 2d, and its embedded image clearly demonstrated that abundant irregularities (PPy/Ag NPs) have been attached onto the surfaces of the fabric fibers. Meanwhile, the macro-knitting structure and pore channels between the fibers were reserved (Fig. 2c), which ensured that air and liquid could pass through. The roughness of the fabric before and after loading PPy/Ag NPs has been analyzed based on the Wenzel equation (eqn (1)) and the Cassie–Baxter equation (eqn (2)):

$$\cos\theta_w = r\frac{\gamma_{sg}-\gamma_{sl}}{\gamma_{lg}} = r\cos\theta \quad (1)$$

$$\cos\theta_c = f_s(\cos\theta + 1) - 1 \quad (2)$$

In which θ_w (or θ_c) and θ are the WCA values on the rough and smooth surfaces, respectively, and r is the roughness factor defined as the ratio of the actual surface area of the rough surface to the geometric projected area, which is always larger than 1. Moreover, f_s and $1 - f_s$ are the fractions of the solid contact area and air contact area with water, respectively. Table 1 showed the calculated data through eqn (1) and (2) according to the wetting properties of the OTS modified fabric samples before and after loading the PPy/Ag NPs. Specifically, the OTS modified fabric after loading the PPy/Ag NPs (PPy/Ag/OTS-fabric) became superhydrophobic with a WCA of 159° (Fig. 1a), and its roughness factor and the fraction of air in contact with water were 3.39 and 90.88%, respectively. In comparison, the roughness factor and fraction of air in contact with water of the OTS modified fabric without loading with PPy/Ag NPs were just 3.04% and 77.73%, respectively. Apparently, much more air was trapped into the PPy/Ag/OTS-fabric under the water droplet than in the OTS modified fabric. This firmly demonstrated that the presence of the PPy/Ag NPs did indeed increase the fabric roughness, which had a significant effect on the wetting properties of the fabric surface. Furthermore, the WCA of the original fabric composed of PU fibers was 130°, which was much lower than that with OTS modification (147°), indicating the significance of selecting materials with an appropriate surface energy as well.

Table 1 Calculated data based on the Wenzel equation and the Cassie–Baxter equation

	Wenzel model			Cassie model			
Sample name	θ_w	θ	r	θ_c	θ	f_s	$1 - f_s$
Smooth OTS film		106°			106°		
OTS modified fabric	147°		3.04	147°		22.27%	77.73%
PPy/Ag/OTS-fabric	159°		3.39	159°		9.12%	90.88%

The FTIR spectra and the corresponding data of the coatings on the three types of fabric specimens containing PPy, Ag or OTS are provided in Fig. 3 and Table 2. In the high frequency region, the strong absorption peak at 3424 cm^{-1} stems from the N–H stretching vibration, meanwhile, two absorption peaks at 2846 and 2925 cm^{-1} were attributed to the asymmetric stretching vibration and symmetric stretching vibration of $-CH_2$.[21] In addition, the stretching vibrations of C=N, C=C, C–C and C–N in the pyrrole ring were observed at 1632, 1540, 1453 and 1380 cm^{-1} in all three spectra.[22] Apparently, PPy successfully combined with the fabric specimen in the first step. In the spectra of the coatings after the loading of AgNPs, the absorption peak at 2356 cm^{-1} (C–H stretching vibration) split into two peaks, which could be attributed to the reaction as described in Fig. 1a. Furthermore, the characteristic peaks at 1342 cm^{-1} (O–H bending vibration), 968 cm^{-1} (bending vibration of Si–OH), 781 cm^{-1} (stretching vibration of Si–C) and 725 cm^{-1} (bending vibration of out-of-plane $-(CH_2)_n-$, $n \geq 4$) fully demonstrated that the OTS had been grafted onto the PPy/Ag-fabric successfully (Fig. 1b).[23,24]

The original spandex fabric has a certain hydrophobicity. After loading PPy/Ag NPs using the *in situ* polymerization

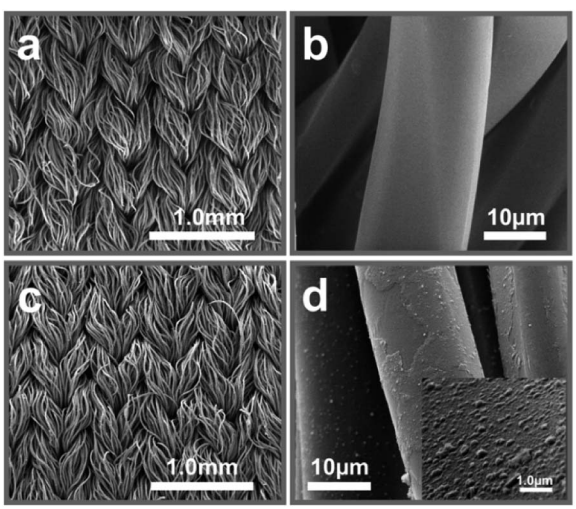

Fig. 2 SEM images of (a) and (b) an original specimen and (c) and (d) the PPy/Ag NPs loading specimen. The inset in (d) is the magnified image of the PPy/Ag NPs loading fiber.

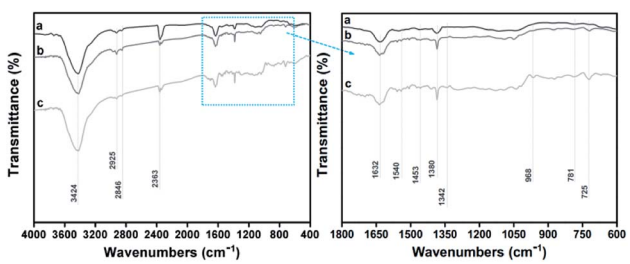

Fig. 3 FTIR spectra of the coatings on different fabric specimens: (a) PPy, (b) PPy/Ag, and (c) PPy/Ag/OTS.

Table 2 Wavenumbers and attributions of the characteristic peaks in the FTIR spectra

Wavenumber (cm^{-1})	Attribution of the characteristic peaks
3424	N–H stretching vibration
2925	Asymmetric stretching vibration of $–CH_2$
2846	Symmetric stretching vibration of $–CH_2$
2363	C–H stretching vibration
1632	C=C, C=N stretching vibration
1540	C–C stretching vibration in pyrrole ring
1453	C–N stretching vibration in pyrrole ring
1380	C–N stretching vibration
1342	O–H bending vibration
968	Bending vibration of Si–OH
781	Stretching vibration of Si–C
725	Bending vibration of out-of-plane $–(CH_2)_n–$, $n \geq 4$

method, the PPy/Ag-fabric specimen gained superhydrophilicity and underwater superoleophobicity (Fig. 4a and b). As we have proved before, the material and surface roughness are the key factors affecting the wetting behavior of the substrate. Apparently, the PPy/Ag NPs coating significantly increases the surface energy and roughness of the fabric specimen. When it was immersed in water, the oil droplets could stand on its surface with an underwater oil contact angle (OCA) of 160° (Fig. 1a and 4b). During attempts to separate the chloroform-in-water emulsion, the PPy/Ag-fabric was wet with the water phase, and the feed was slowly filtered owing to gravity, and then fell into the measuring cylinder (Fig. 4d). Finally, the foggy cloudy liquid became clarified and transparent (Fig. 4c), and the micron oil droplets completely disappeared under the optical microscope (Fig. 4c_0 and c_1). After careful evaluation and calculation, the separation efficiency and flux of the PPy/Ag-fabric for the chloroform-in-water emulsion were found to be 99.79% and 682.14 L m^{-2} h^{-1}, respectively. On the basis of loading the PPy/Ag NPs, OTS modification was further carried out, and the as-obtained PPy/Ag/OTS-fabric became superhydrophobic and superoleophilic (Fig. 4e and f). This is because the existence of OTS largely reduced the surface energy of the fabric specimen. Moreover, this PPy/Ag/OTS-fabric also had an outstanding separation effect for the water-in-chloroform emulsion, and its filtration procedure and effects were similar to the former. Specifically, the evenly distributed water droplets in emulsion were successfully removed by the PPy/Ag/OTS-fabric under the observation of an optical microscope (Fig. 4g, g_0 and g_1). With further evaluation and calculation, the separation efficiency and flux of the PPy/Ag/OTS-fabric for the water-in-chloroform emulsion were 96.84% and 1132.34 L m^{-2} h^{-1}, respectively. Except for the water/chloroform emulsions, other mixtures could also be separated using the two fabrics specimens efficiently, for example, the water-in-*n*-hexane emulsion (95.68% and 1003.71 L m^{-2} h^{-1}), methylbenzene-in-water emulsion (99.85% and 721.26 L m^{-2} h^{-1}), and so forth. In conclusion, both the PPy/Ag-fabric and PPy/Ag/OTS-fabric exhibited an excellent separating performance towards different water/oil emulsions, which would satisfy various demands in practical usage, displaying their enormous potential.

The mechanistic diagram for separating opposite types of water/oil emulsions throughout the PPy/Ag-fabric and PPy/Ag/OTS-fabric specimens is presented in Fig. 5. During the separating procedure for the oil-in-water emulsion (or water-in-oil emulsion) using the PPy/Ag-fabric (or PPy/Ag/OTS-fabric) specimen, the water (or oil) wets and penetrates the specimen immediately, as shown in Fig. 5a (or Fig. 5b), while the micron oil (or water) droplets in water (or the oil) phase are rejected by the fabric, which deforms, moves and further coalesces into the larger oil (or water) droplets standing on the top of the specimen. Afterwards, these larger oil (or water) droplets can be easily detached from the PPy/Ag-fabric (or PPy/Ag/OTS-fabric) surface by a simple rinsing treatment. Finally, the oil contaminants were removed (or collected) for subsequent processing.

Owing to the decisive role of the material mechanical stability for practical applications, the friction resistance of the fabric specimens has been evaluated.[25] Specifically, each

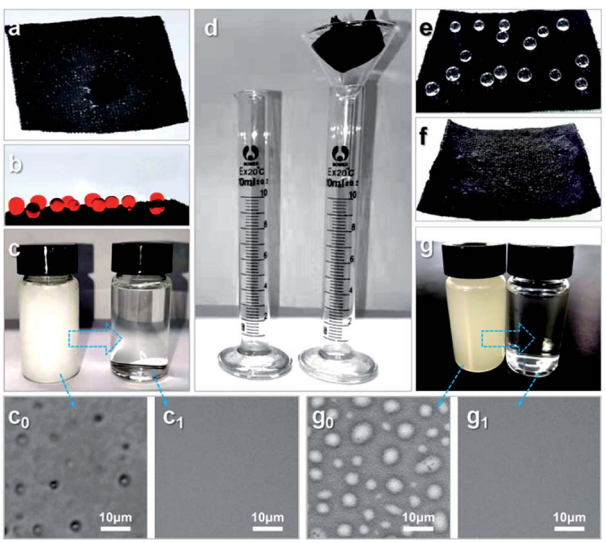

Fig. 4 (a) Water and (b) oil (underwater) droplets on the PPy/Ag-fabric specimen, and (c) a chloroform-in-water emulsion (c_0) before and (c_1) after filtration using the PPy/Ag-fabric specimen. (d) The water/oil filtration procedure, and (e) water and (f) oil droplets on the PPy/Ag/OTS-fabric specimen. (g) A water-in-chloroform emulsion (g_0) before and (g_1) after filtration using the PPy/Ag/OTS-fabric specimen.

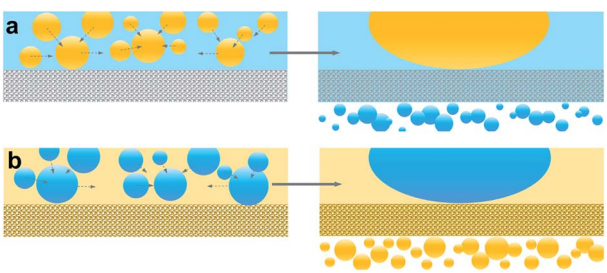

Fig. 5 A diagram showing the separating mechanism of (a) the PPy/Ag-fabric specimen towards an oil-in-water emulsion and (b) the PPy/Ag/OTS-fabric specimen towards a water-in-oil emulsion.

specimen (25 × 25 mm^2) was placed on the original fabric surface, meanwhile, a 100 g weight was settled onto the specimen, which was further moved along with the ruler (200 mm) at a speed of approximately 7 mm s^{-1}. The images of the PPy/Ag- and PPy/Ag/OTS-specimens after 10, 20 and 30 repeated friction test are presented in Fig. 6a and b, which showed that the PPy/Ag- and PPy/Ag/OTS- coatings on the fabrics surfaces were mildly damaged. Fig. 6c shows the wetting performances of the PPy/Ag-specimen and PPy/Ag/OTS-specimen during the increasing number of friction tests with the original fabric. The underwater OCA of the PPy/Ag-fabric was maintained above 150.5° after 15 times and still reached 140° even after 30 times, meanwhile, the WCA in air of the PPy/Ag/OTS-fabric was maintained above 150° after 10 times and still reached 138° even after 30 times. Apparently, the contact angles of both specimens decreased slightly along with the increasing friction times, demonstrating the sufficient roughness and abrasion resistance of the as-prepared PPy/Ag-fabric and the PPy/Ag/OTS-fabric. In addition, the chemical stability of both specimens was also investigated as presented in Fig. 6d. The oleophobic performance of the PPy/Ag-fabric after washing with a strong acid and base did not decrease seriously, and the OCA was always kept above 146°, showing the good underwater superoleophobicity. For the hydrophobic properties of the PPy/Ag/OTS-fabric, its resistance against acids and bases was limited, and was limited to the pH range of 3–12. However, all of the above described results amply proved that the PPy/Ag NPs have indeed been deposited onto the fabric surface steadily using our strategy.

Antibacterial performance is ranked amongst the most attractive features of fabrics modified with conducting polymers and Ag NPs.[26] In this study, three representative bacterial species (*e.g. S. aureus*, *B. subtilis* and *E. coli*) were used for inoculation, and the antibacterial test photographs of the neat original fabric, PPy-fabric, PPy/Ag-fabric and PPy/Ag/OTS-fabric specimens are exhibited in Fig. 7. After cultivation in an incubator for 16 h at 28 °C, numerous indistinct colonies grew on the original fabric and PPy-fabric specimens, as they did not display any antibacterial activity. The PPy/Ag-fabric and PPy/Ag/OTS-fabric specimens showed an outstanding antibacterial activity and an extremely long-lasting antibacterial effect, which could not only kill all of the bacteria in contact with it below, but could also effectively inhibit the growth of surrounding bacteria, especially for the PPy/Ag-fabric specimen. The antibacterial mechanism of the PPy/Ag-based fabrics is derived from the fact that: (i) the external AgNP combines with the hydrosulphonyl in zymoprotein from bacteria tightly to make the protein coagulate and destroy its cellular synthase activity, depriving it of the ability to proliferate and develop; (ii) then the Ag^+ is dissolved and further combines with the bacterial membrane protein, causing the leakage of matter within the membrane; and (iii) the Ag^+ also impedes the synthesis of peptidoglycan and repair of the cell wall, effectively killing the *B. subtilis*, *S. aureus* and *E. coli*.[27] Most importantly, the Ag^+ dissociates from the inactivated thallus and continues its bactericidal activity. However, their antibacterial activities are different. Apparently, the introduction of OTS prevented the releasing of external AgNP from fabric specimens in the culture medium (water system). Furthermore, their inhibitory activities against different bacterial species were different as well, showing *B. subtilis* (Gram positive), *S. aureus* (Gram positive) and *E. coli* (Gram negative) in descending order. This indicated that our fabric products had a better antibacterial effect towards Gram positive bacteria. The main reason for this is that the outer membrane of Gram negative bacteria contains lipopolysaccharide, which can retard the sterilization effect of Ag/Ag^+ towards bacteria.

To explore the conductivity intuitively, the fabric specimens before and after loading PPy/Ag NPs were respectively introduced into a closed loop including two batteries (1.5 V), a light-emitting diode (LED) and several wires. In this loop, the current flowed through the LED from the P-pole to the N-pole, while the

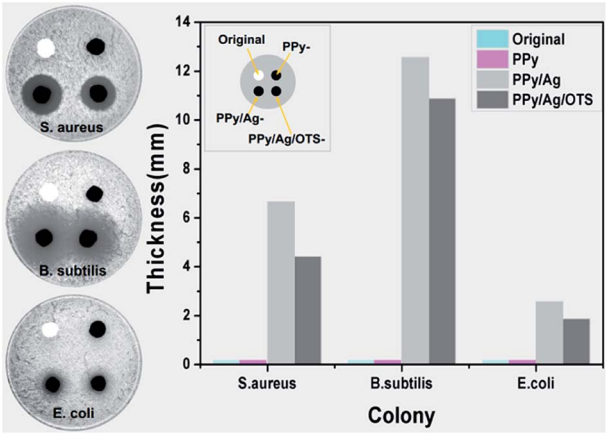

Fig. 7 Photographs and antibacterial loop data for fabric specimens placed on a peptone plate inoculated with *S. aureus*, *B. subtilis*, and *E. coli*.

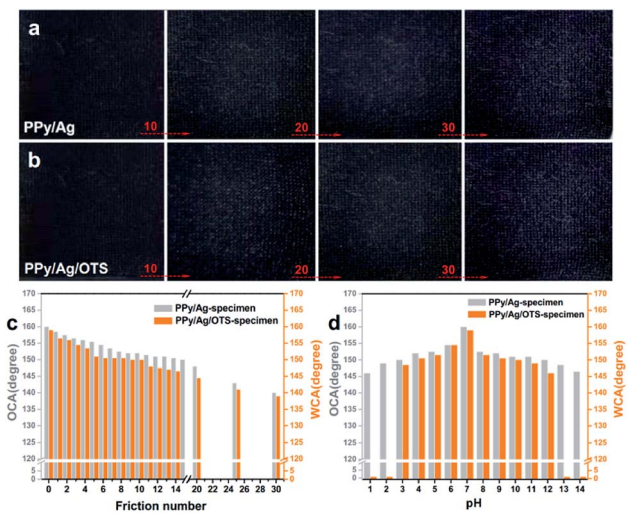

Fig. 6 Photographs of (a) PPy/Ag- and (b) PPy/Ag/OTS-specimens after 10, 20 and 30 repeat friction tests. Superwetting durability: (c) abrasion resistance against the original fabric and (d) the resistance of the PPy/Ag-specimen (OCA underwater) and PPy/Ag/OTS-specimen (WCA in air) towards acids and bases.

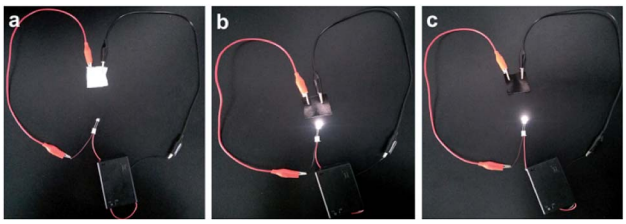

Fig. 8 Photographs of (a) original fabric, (b) PPy/Ag-fabric and (c) PPy/Ag/OTS-fabric specimens in a closed loop.

electrons flowed from the N-pole to the P-pole. To confront the sudden energy level variation, these electrons can release the extra energy, and the energy difference is converted into photons, leading to a luminous effect.[28] Apparently, the introduction of the original fabric could not light up the LED in the loop (Fig. 8a), while the as-prepared PPy/Ag- and PPy/Ag/OTS-fabrics could (Fig. 8b and c), indicating the good electrical conductivity of our fabric products. Predictably, when the electrical power was applied, these fabric membranes can acquire a better bactericidal activity during oil/water separation owing to the electroporation effect, and the wet membranes after filtration can be dried more rapidly than those without conductivity owing to the thermal effect of the current.

Conclusions

In summary, a feasible and simple strategy has been proposed to fabricate multifunctional knitted fibrous membranes with superwetting, antibacterial and conductive properties. A PPy/Ag NPs coating has been successfully attached to the surface of the spandex fabric using *in situ* redox-oxidation polymerization. The contact angle results showed that the WCA in air and the underwater OCA of the PPy/Ag-fabric specimen were 0° and 160°, respectively. After further OTS grafting, the above specimen displayed a WCA in air and an underwater OCA of 159° and 160°, respectively. Both types of membranes exhibited outstanding special wetting behaviors, which completely allowed the removal and collection of organic contaminants from oil-in-water and water-in-oil emulsions. Separation experiments further verified the remarkable filtration effects of both the fabric membranes. The abrasion evaluation results showed that both specimens still maintained an underwater OCA and WCA in air of around 140° even after the application of friction dozens of times. Moreover, the PPy/Ag-fabric membrane showed better resistance against bases and acids than the PPy/Ag/OTS-fabric membrane, while both membranes possessed outstanding electrical conductivity and antibacterial activity towards *S. aureus*, *B. subtilis*, and *E. coli*, especially the PPy/Ag-fabric membrane. This strategy for achieving multifunctional fabric membranes could offer a certain theoretical reference for the designers of functional and intelligent fibrous membrane materials.

Conflicts of interest

There are no conflicts to declare.

Acknowledgements

The research was supported by the Key Laboratory of Bio-based Material Science & Technology (Northeast Forestry University, Ministry of Education) (SWZ-MS201910), the Project of Jilin Province Science and Technology Development Research (20190103110JH), the State Key Laboratory of Bio-Fibers and Eco-Textiles (Qingdao University) (K2019-08), the National Natural Science Foundation of China (31971616), the Science and Technology Innovation Development Plan of Jilin City (201830811) and the Fundamental Research Funds for the Wood Material Science and Engineering Key Laboratory of Jilin Province.

Notes and references

1 P. Bober, J. Stejskal, I. Šeděnková, M. Trchová, L. Martinková and J. Marek, The deposition of globular polypyrrole and polypyrrole nanotubes on cotton textile, *Appl. Surf. Sci.*, 2015, **356**, 737.
2 Y. Kim, L. T. Mccoy, E. Lee, H. Lee, R. Saremi, C. Feit, I. R. Hardin, S. Sharma, S. Mani and S. Minko, Environmentally sound textile dyeing technology with nanofibrillated cellulose, *Green Chem.*, 2017, **19**, 4031.
3 J. Singh, P. Shrivastava, K. Mukophadhyaya, D. Prasad and V. Sharma, Design and development of composite nonwoven filter for pre-filtration of textile effluents using nano-technology, *J. Mater. Sci. Eng.*, 2017, **6**, 3.
4 Y. L. Jiang, M. Togane, B. L. Lu and H. Yokoi, sEMG sensor using polypyrrole-coated nonwoven fabric sheet for practical control of prosthetic hand, *Front. Neurosci.*, 2017, **11**, 33.
5 J. Xu, D. X. Wang, L. L. Fan, Y. Yuan, W. Wei, R. N. Liu, S. J. Gu and W. L. Xu, Fabric electrodes coated with polypyrrole nanorods for flexible supercapacitor application prepared *via* a reactive self-degraded template, *Org. Electron.*, 2015, **26**, 292.
6 Z. Yang, *The functionalization of natural wood and its application in water treatment*, Academic Dissertation of Lanzhou University, 2019.
7 W. Barthlott, M. Mail, B. Bhushan and K. Koch, Plant surfaces: structures and functions for biomimetic innovations, *Nano-Micro Lett.*, 2017, **9**, 116–155.
8 S. Yang, X. Jin, K. Liu and L. Jiang, Nanoparticles assembly-induced special wettability for bio-inspired materials, *Particuology*, 2013, **11**, 361.
9 X. Li, G. Wei, M. A. Benjamin, K. S. Reese, D. W. William and L. P. Derek, Rational design of superhydrophilic/superoleophobic surfaces for oil–water separation *via* thiol-acrylate photopolymerization, *ACS Omega*, 2018, **3**, 10278.
10 T. A. Otitoju, A. L. Ahmad and B. S. Ooi, Superhydrophilic (superwetting) surfaces: a review on fabrication and application, *J. Ind. Eng. Chem.*, 2017, **47**, 19.
11 C. Zhang, P. Li and B. Cao, Electrospun microfibrous membranes based on PIM-1/POSS with high oil wettability for separation of oil-water mixtures and cleanup of oil soluble contaminants, *Ind. Eng. Chem. Res.*, 2015, **54**, 8772.

12 M. N. Qu, X. R. Ma, J. M. He, J. Feng, S. S. Liu, Y. L. Yao, L. G. Hou and X. R. Liu, Facile selective and diverse fabrication of superhydrophobic, superoleophobic-superhydrophilic and superamphiphobic materials from Kaolin, *ACS Appl. Mater. Interfaces*, 2017, **9**, 1011.
13 C. Zhang, P. Li and B. Cao, Fabrication of superhydrophobic-superoleophilic fabrics by an etching and dip-coating two-step method for oil-water separation, *Ind. Eng. Chem. Res.*, 2016, **55**, 5030.
14 Z. Shami, S. M. Amininasa and P. Shakeri, Structure-property relationships of nanosheeted 3D hierarchical roughness MgAl-layered double hydroxide branched to an electrospun porous nanomembrane: a superior oil-removing nanofabric, *ACS Appl. Mater. Interfaces*, 2016, **8**, 28964.
15 L. X. Li, J. P. Zhang and A. Q. Wang, Removal of organic pollutants from water using superwetting materials, *Adv. Sci.*, 2018, **18**, 118.
16 M. N. Qu, L. L. Ma, Y. C. Zhou, Y. Zhao, J. X. Wang, Y. Zhang, X. D. Zhu, X. R. Liu and J. M. He, Durable and recyclable superhydrophilic-superoleophobic materials for efficient oil/water separation and water-soluble dyes removal, *ACS Appl. Nano Mater.*, 2018, **1**, 5197.
17 C. Sciancalepore, F. Moroni, M. Messori and F. Bondioli, Acrylate-based silver nanocomposite by simultaneous polymerization-reduction approach *via* 3D stereolithography, *Compos. Commun.*, 2017, **6**, 11.
18 S. H. Mir, K. Ebata, H. Yanagiya and B. Ochiai, Alignment of Ag nanoparticles with graft copolymer bearing thiocarbonyl moieties, *Microsyst. Technol.*, 2017, **24**, 605–611.
19 N. Guan, P. Chew, Y. J. Zhang, K. L. Goh, J. S. Ho, R. Xu and R. Wang, Hierarchically structured Janus membrane surfaces for enhanced membrane distillation performance, *ACS Appl. Mater. Interfaces*, 2019, **11**, 25524.
20 K. M. Zepon, M. S. Marques, M. M. S. Paula, F. D. P. Morisso and L. A. Kanis, Facile, green and scalable method to produce carrageenan-based hydrogel containing in situ, synthesized AgNPs for application as wound dressing, *Int. J. Biol. Macromol.*, 2018, **113**, 51.
21 C. Y. Wang, C. Piao and C. Lucas, Synthesis and characterization of superhydrophobic wood surfaces, *J. Appl. Polym. Sci.*, 2011, **19**, 1667.
22 M. Trchová, Z. Morávková, I. Šeděnková and J. Stejskal, Spectroscopy of thin polyaniline films deposited during chemical oxidation of aniline, *Chem. Pap.*, 2012, **66**, 415.
23 N. Lv, X. L. Wang, S. T. Peng, L. Luo and R. Zhou, Superhydrophobic/superoleophilic cotton-oil absorbent: preparation and its application in oil/water separation, *RSC Adv.*, 2018, **8**, 30257.
24 C. S. Sevov, R. E. M. Brooner, E. Chénard, R. S. Assary, J. S. Moore, J. R. López and M. S. Sanford, Evolutionary design of low molecular weight organic anolyte materials for applications in nonaqueous redox flow batteries, *J. Am. Chem. Soc.*, 2015, **137**, 14465.
25 C. J. Wei, F. Y. Dai, L. G. Lin, Z. H. An, Y. He, X. Chen, L. Chen and Y. P. Zhao, Simplified and robust adhesive-free superhydrophobic SiO_2-decorated PVDF membranes for efficient oil/water separation, *J. Membr. Sci.*, 2018, **17**, 33001.
26 N. Maráková, P. Humpolíček, V. Kašpárková, Z. Capáková, L. Martinková, P. Bober, M. Trchová and J. Stejskal, Antimicrobial activity and cytotoxicity of cotton fabric coated with conducting polymers, polyaniline or polypyrrole, and with deposited silver nanoparticles, *Appl. Surf. Sci.*, 2017, **369**, 169.
27 S. Rajeshkumar, C. Malarkodi, M. Vanaja and G. Annadura, Anticancer and enhanced antimicrobial activity of biosynthesizd silver nanoparticles against clinical pathogens, *J. Mol. Struct.*, 2016, **1116**, 165.
28 A. Bergantini, M. J Abplanalp, P. Pokhilko, A. I. Krylov, C. N. Shingledecker, E. Herbst and R. I. Kaiser, A combined experimental and theoretical study on the formation of interstellar propylene oxide (CH_3CHCH_2O)-a chiral molecule, *Astrophys. J.*, 2018, **860**, 108.

